PROCEEDINGS OF SPIE

SPIEDigitalLibrary.org/conference-proceedings-of-spie

Innervation of the cow's inner ear derived from micro-computed tomography

Loic Costeur
Bastien Mennecart
Anna Khimchenko
Bert Müller
Georg Schulz

SPIE.

Innervation of the cow's inner ear derived from micro-computed tomography

Loïc Costeur[a*], Bastien Mennecart[a], Anna Khimchenko[b], Bert Müller[b], and Georg Schulz[b]
[a] Naturhistorisches Museum Basel, Augustinergasse 2, 4001 Basel, Switzerland;
[b] Biomaterials Science Center, University of Basel, Gewerbestrasse 14, 4123 Allschwil, Switzerland;

ABSTRACT

The innervation of the inner ear has been thoroughly investigated in humans and in some animal models such as the guinea pig, the rabbit, the cat, the dog, the rat, the pig and some monkeys. Ruminant inner ears are still poorly known and their innervation was never investigated despite its potential interest in phylogenetic reconstructions. Following earlier works on the ontogeny of the cow's ear, we expand our understanding of this structure by reconstructing the fine innervation pattern of the inner ear of the cow in two ontogenetic stages, at 7 months gestation and at an adult age. Since we work on dry skeletal specimens, only the endocast of the innervation inside the petrosal bone was reconstructed up to the internal acoustic meatus. The paths of the facial and vestibulocochlear nerves could be reconstructed together with that of the spiral ganglion canal. The nerves have a very fibrous pattern. The bony cavities of the ampular and utricular branches of the vestibulocochlear nerve could also be reconstructed. Our observations confirm that not all bony structures are present in foetal stages since the branch of cranial nerve VII is not visible on the foetus but very broad on the adult stage. The fibrous pattern within the modiolus connecting the spiral canal to the cochlear nerve is also less dense than in the adult stage. The shape of the branch of cranial nerve VII is very broad in the cow ending in a large hiatus Fallopii; this, together with the above-mentioned particularities, could constitute relevant observations for phylogenetical purposes when more data will be made available.

Keywords: microtomography, laboratory X-ray source, absorption contrast, Ruminantia, inner ear, spiral ganglion, nerves, veins, cochlea.

1. INTRODUCTION

The anatomy of the vascular system irrigating and innervating the inner ear is well known in a range of mammals including the man and some primates, some rodents like the guinea pig, or carnivores like the cat. (e.g., [1-5]). These studies investigated the arrangement of blood vessels irrigating the cochlea. Numerous works starting with the seminal Gray's Anatomy [6] or the later work of Fleischer [7] detailed description of the cochlea and surrounding structures of the modiolus, the inner part of the cochlea, in several mammals paved the way of our understanding of this highly complex structure where blood vessels, arteries, nerves, and their corresponding fibers and cells build afferent and efferent interrelated networks inside a tiny area of less than half a millimeter even in the largest mammals. Most of these studies are based on histological slides or prepared soft structures that enabled the authors to represent the structures in 2D, mostly as interpretative drawings, and sometimes as pictures of slides. The advent of 3D techniques such as micro-computed tomography makes it possible to represent the innervation of the inner ear in 3D and show its connexion to the inner ear itself. The passage of the nerves inside the petrosal bone, leaving cavities in the bone, and their contacts with the inner ear are comparatively relatively poorly known and have never been investigated through the ontogeny in mammals outside in humans. While the mammalian inner ear itself, or its endocast the bony labyrinth, has been thoroughly studied in the past years, both morphologically and ontogenetically using 3D computed tomography produced data (e.g., [8-15]), its innervation, by means of imaging the cavities left by nerves and veins, has received little interest and only a handful of fossil mammals have been published in this respect (e.g., [16-18]). The information coming from this structure have, until now, mostly concerned pure morphology and broad scale comparisons among early therians and eutherians except in the case of [16] where a fossil mammal inner ear, that of the Jurassic *Dryolestes*, provides information on the evolution of the cochlea itself: the complex mammal-type innervation of the cochlea precedes its coiling in mammalian evolution.

* loic.costeur@bs.ch; phone: +41 61 266 55 87

Developments in X-Ray Tomography XI, edited by Bert Müller, Ge Wang, Proc. of SPIE Vol. 10391,
103911I · © 2017 SPIE · CCC code: 0277-786X/17/$18 · doi: 10.1117/12.2276158

Because of this and because the inner ear ossifies early in the development of a mammal such as exemplified in ruminants [15], the innervation pattern could be a source of pertinent characters for phylogenetic reconstructions. A quick comparative look at the nicely reconstructed innervation in an early ungulate *Protungulatum* [17] or in the anoplotheriid *Diplobune* [18] shows significant differences in the coiling of the spiral canal or the shape and length of the branch for cranial nerve VII. In light of the very few data available, it is still hard to use this information in phylogenies but adding observations in other taxa will undoubtedly lead to a better understanding of the structure and of its potential for phylogeny, or maybe even for evolutionary studies such as in the study of Mourlam and Orliac [19].

Here we describe the bony cavities of the innervation of the inner ear of the modern cow (*Bos taurus*, Bovidae, Ruminantia, Mammalia) both in an adult stage and in a fetal stage at about 6 months gestation. We use micro computed tomography to generate high resolution images of the bony labyrinth and its surrounding structures and providing flexible 3D renderings. We aim at expanding the knowledge of the inner and middle ear ossification timing previously acquired on the same species and using the same specimens [15, 20]. This work constitutes the first steps of a comparative dataset on extant artiodactyls and will hopefully constitute a starting point in generating 3D data for comparative purposes.

2. MATERIALS AND METHODS

2.1 Specimen preparation and methods

We CT-scanned and digitally segmented the innervation of the bony labyrinth of specimens NMB 3367, a ca. 165 days old cow foetus (species *Bos taurus*) and NMB 1037, an adult cow. Age estimate was done following [15]. The specimens are a dry skeletal skull and a petrosal bone manually extracted from a skull, respectively. They thus both give access to endocasts (hollow spaces) of soft structures that are otherwise not preserved anymore. They both were previously published after their bony labyrinth was reconstructed [15]).

The endocasts of the innervations were segmented and reconstructed using AVIZO LITE 9.0. Nomenclature follows [21] and [18]. As explained here we reconstructed the endocasts of the innervations but we will refer throughout the text to the soft structures nomenclature in order to relate the cavities to the structures that left them within the bone. So no soft structure is directly visible and described here, but rather its endocast within the petrosal bone.

2.2 X-Ray microtomography

Micro computed tomography is a powerful non-destructive tool for a wide range of scientific applications [22 - 25]. The X-ray microtomography measurements were performed using an advanced, commercially available nanoCT® system nanotom® m (phoenix x-ray, GE Sensing & Inspection Technologies GmbH, Wunstorf, Germany), which is equipped

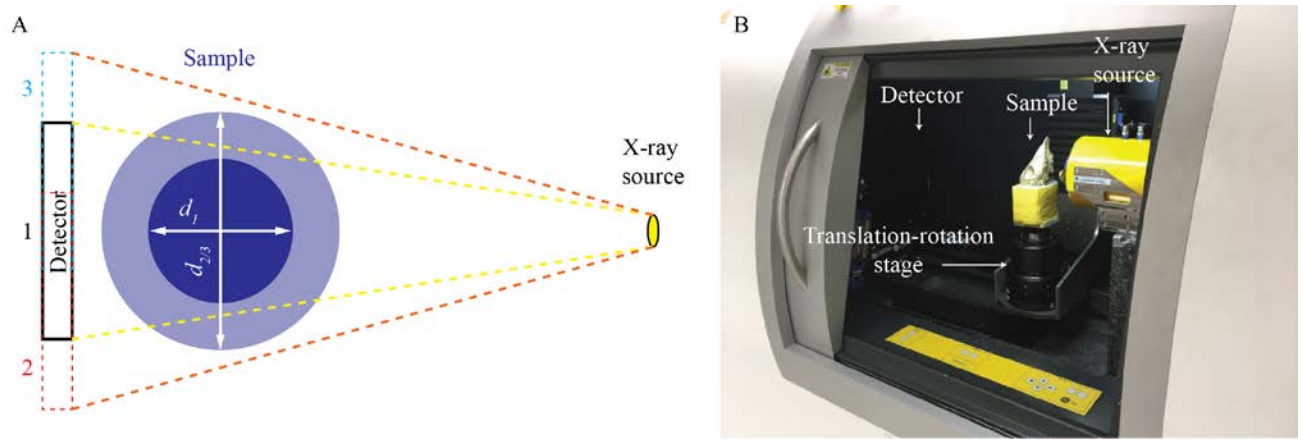

Figure 1. Schema (A) and photograph (B) of the experimental setup used for microtomography measurements. For the imaging experiments, a sample up to d_1 = 240 mm in diameter is positioned on the translation-rotation stage downstream from the X-ray source and imaged on the detector (detector position 1). To increase the field of view for a bigger sample ($d_{2/3}$), the 1.5-fold virtually extended detector can be used (detector positions 2 - 3). For the photo, specimen NMB 3367, a ca. 165 days old cow foetus (species *Bos taurus*) was used.

with a 180 kV / 15 W high-power nanofocus (HPNF) X-ray source with tungsten (W) transmission target optimized for a long-term stability with an adjustable focal spot diameter (0.9 – 2.7 µm) and temperature stabilized digital GE DXR 500L detector based on based endurance™ scintillator technology [26, 27], see Figure 1. For the imaging experiments, a sample was positioned on the translation-rotation stage downstream from the X-ray source and imaged on the flat panel detector. This detector has 3072 × 2400 pixels with a pixel size of 100 µm. To increase the field of view for a bigger sample, the 1.5-fold virtually extended detector can be used.

During 1440 equiangular radiographs were taken over 360°. In order to image the specimens an accelerating voltage of 120 kV and a beam current of 200 µA were used where the mean photon energy was increased by adding a 0.25 mm Cu filter. The measurements were taken in the tube operation mode *"0"* with an estimated focal spot diameter of 2.7 µm, as specified by the supplier. The whole scanning time of one specimen took about 2 hours. The camera readout resulted in a pixel length of 35 µm for NMB 3367 and 45 µm for NMB 1037.

Data processing and reconstruction were done automated using the datos|x 2.0 software (phoenix x-ray, GE Sensing & Inspection Technologies GmbH, Wunstorf, Germany), which implements cone beam reconstruction based on Feldkamps algorithm [28].

3. RESULTS

3.1 Inner ear in a foetus cow

Figure 2 shows the innervation of the cow inner ear in a foetus cow. The spiral canal constituted by the spiral ganglions runs around the modiulus of the cochlea in a tight manner giving a tubular shape to the structure that is surrounding the

cochlear nerve located inside it. The canal itself is long and tightly coiled, with about 3 turns recorded, and has a relatively broad diameter indicating relatively large spiral ganglions. Broad and spaced fibers connect it to the cochlearnerve in a radiating pattern. It is branched within the primary bony lamina inside the cochlea, so at the limit of the scala vestibuli and scala tympani. The ampullar branch of cranial nerve VIII, the vestibulocochlear nerve, is thick and round in diameter, and reaches the anterior ampulla. Its saccular branch is partly visible while its utricular branch is still not ossified and could thus not be reconstructed. The same is true with the branch of the cranial nerve VII, or facial nerve, which usually enters the petrosal bone through the hiatus Fallopii. The latter is not yet ossified and most of the bony tract for the facial nerve lacks on the reconstruction. The internal acoustic meatus opens in a round shape on top of the modiolus and constitute the entrance of the vestibulocochlear nerve into the petrosal bone.

3.2 Inner ear in an adult cow

Figure 3 shows the innervation of the cow inner ear in an adult cow. The spiral canal is similar as in the foetus; it is tight and completes about 3 turns. It is longer and reaches more dorsally inside the basal turn of the cochlea. Together with the endocast of the cochlear nerve, they constitute a tubular shape that constitutes most of the volume of the modiolus. The spiral ganglions are relatively large inducing a thick spiral canal. As in the foetus, fibers run within the modiolus between the spiral canal and the cochlear nerve but they are here less spaced or more vascularisation is present between the larger fibers so that the walls of the spiral look very densely innervated. The basal turn of the spiral canal is also broader than in the foetus. The ampullar branch of cranial nerve VIII, the vestibulocochlear nerve, is thick and round in diameter, and reaches the anterior ampulla. Both the utricular and saccular branches are well visible, the former being a thick and circular canal (here only partly reconstructed). The branch for cranial nerve VII is very large, very thick and ends in a broad hiatus Fallopii. The internal acoustic meatus opens in an ellipsoid shape on top of the modiolus and constitute the entrance of the vestibulocochlear nerve into the petrosal bone; it occupies a large surface.

4. DISCUSSION

4.1 Cranial nerve pathways and spiral canal of the cochlea

The tracts of both cranial nerves VII and VIII and of the spiral canal containing the spiral ganglions could be reconstructed with the use of micro-computed tomography data. Cranial nerve VII is the facial nerve and it is recorded here through the tract of one of its branches, namely that of the greater petrosal nerve entering the petrosal bone through the hiatus Fallopii. It innervates the lacrimal gland. Cranial nerve VIII is the vestibulocochlear nerve, or auditory

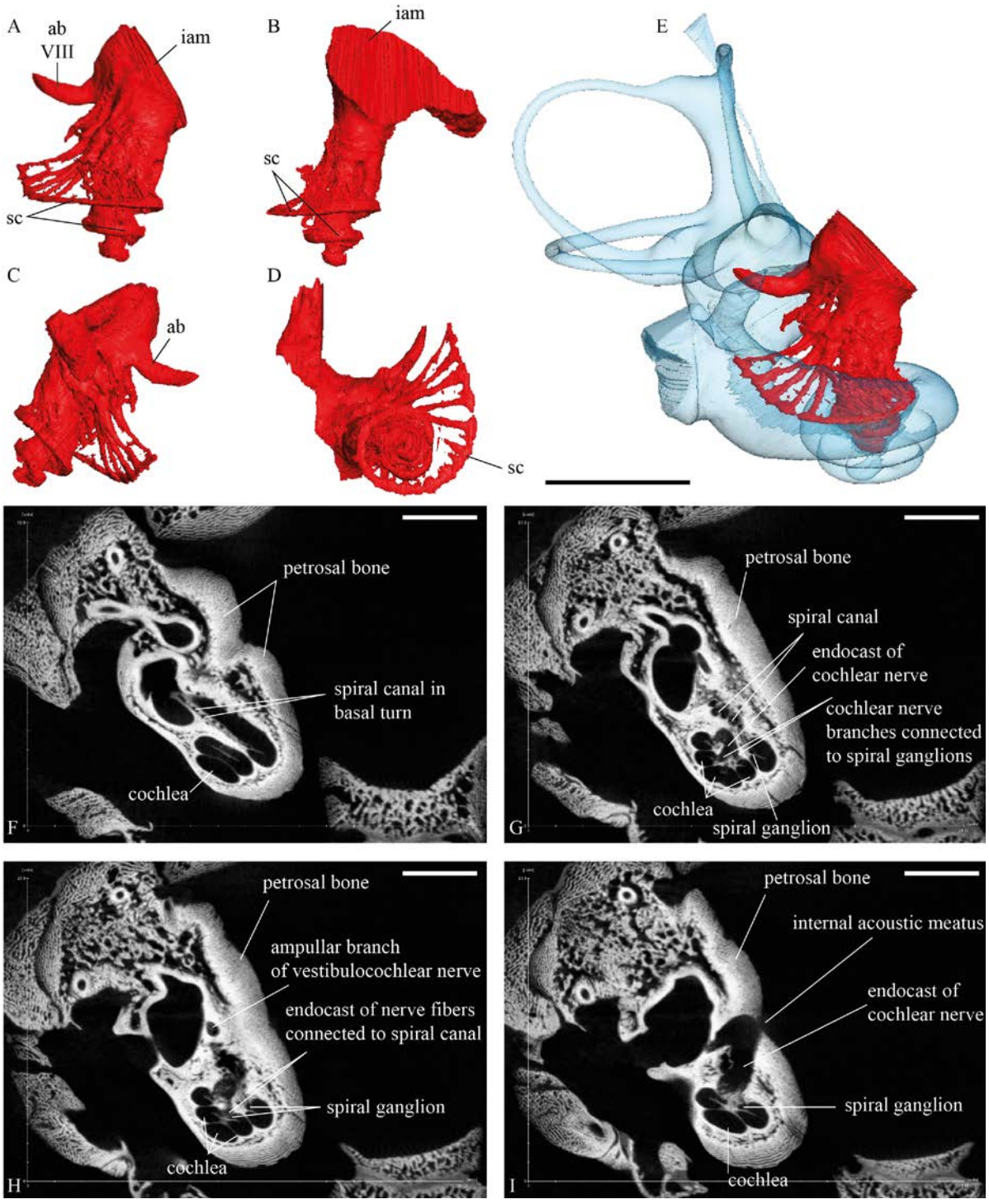

Figure 2. Innervation of the cow inner ear in a foetus cow; A, ventromedial; B, dorsomedial; C, anterolateral; D, ventrolateral views; E, posteromedial view in connexion with the inner ear rendered transparent; F - I: computed-tomography slices perpendicular to the basal-apical axis of the cochlea. Abbreviations: ab, ampullar branch of vestibulocochlear nerve (VCN); hf: hiatus Fallopii; iam, internal acoustic meatus; sb -VIII, saccular branch of the VCN; sc, spiral canal; ub -VIII, utricular branch of the VCN; VII, facial nerve VII; VIII, vestibulocochlear nerve (VCN). Scale bar 5 mm.

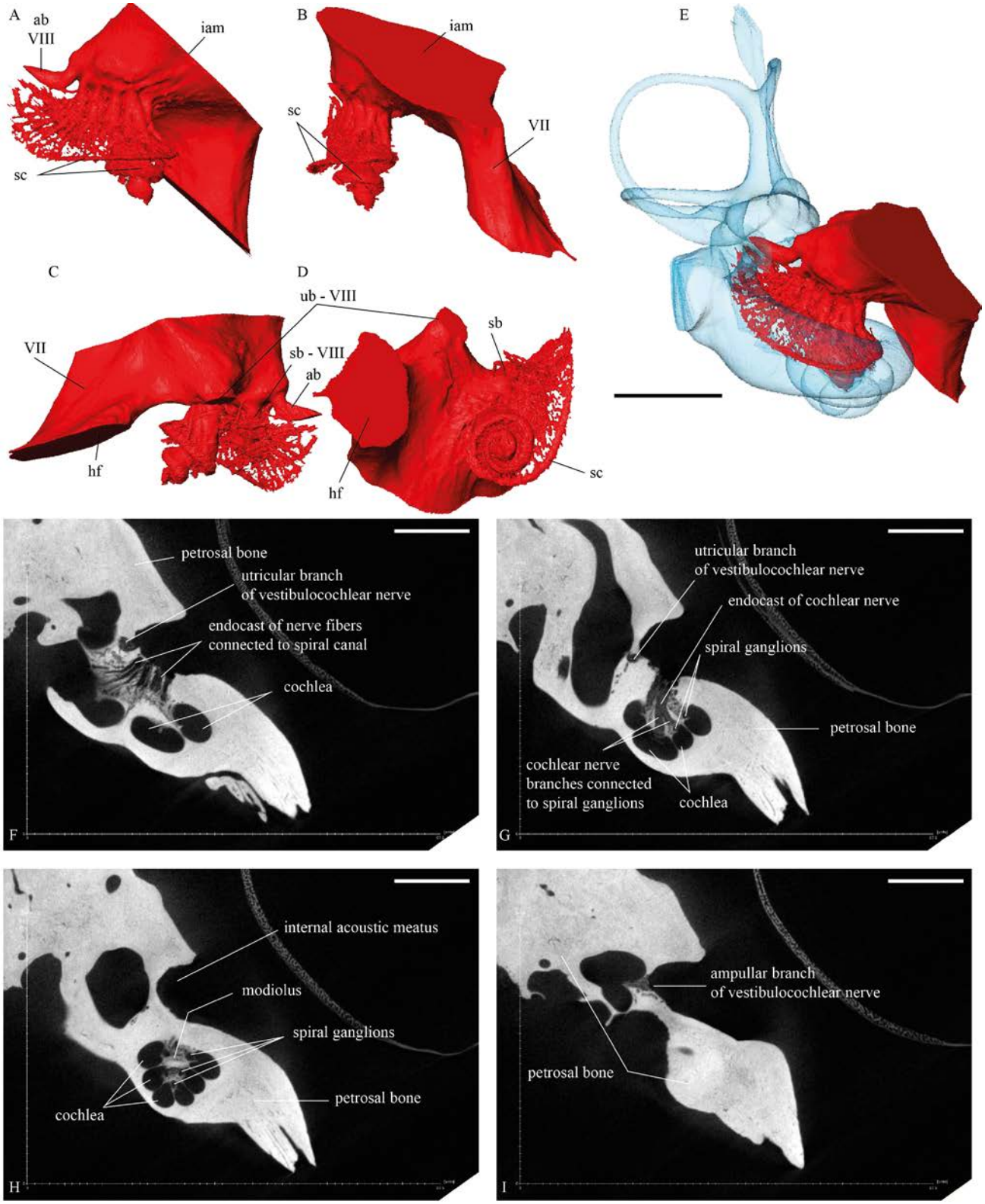

Figure 3. Innervation of the cow inner ear and adult cow; A, ventromedial; B, dorsomedial; C, anterolateral; D, ventrolateral views; E, posteromedial view in connexion with the inner ear rendered transparent; F - I: computed-tomography slices perpendicular to the basal-apical axis of the cochlea. See figure 2 for abbreviations. Scale bar 5 mm.

vestibular nerve, innervates the cochlea and vestibule in the inner ear and thus transmits the auditory and balance information to the brain. It has several branches within the petrosal bone, the main one is the cochlear nerve running in the cochlear cavity, the modiolus, and connected to the spiral ganglions. The other branch is the vestibular nerve separated in smaller branches, which are connected to the ampullae of the semi-circular canals as well as to the maculae of the utricule and saccule (the utricular and saccular branches seen in Fig. 3). The spiral canal is constituted by the spiral ganglions, which are filled with bipolar cells that are connected to the hair cells of the organ of Corti within the cochlear duct. They thus transmit the information to the cochlear nerve fibers. It is not yet clear how specific these structures and their tracts within the petrosal bone are and if they can be used to investigate both the phylogenetic relationships of extinct species and features of their ecology such as hearing frequencies or locomotor capabilities. A comparison with published data on fossil artiodactyls, the group in which ruminants, and thus the cow, are included [17, 18], shows strong differences. While all the features are present, their shape, tracts and arrangement are different. The pathway for the branch of the facial nerve is much thicker in the adult cow than in the very few "ungulate" specimens where it is known (*Protungulatum* and *Diplobune*). The shape of the ampullar branch of the vestibular nerve is also markedly different, being here much thicker and circular in diameter than in *Diplobune* for example [18]. The spiral of the spiral canal is also different depending on the shape of the cochlea that has been shown to be of phylogenetic relevance in deer, which are artiodactyls related to the cow [29]. It is longer and more tightly coiled than in *Diplobune* or *Protungulatum*. Less fibers radiating into the primary bony lamina were visible on our specimens than on both above-mentioned fossil taxa and the utricular branch of the vestibular nerve is more protruding than in those two species and sits directly above the branch for the cochlear nerve, which is very much different than in *Diplobune* [18]. 3D reconstructions of the innervation pattern in artiodactyls, and in particular for ruminants, are otherwise unknown for living species making this work the first comprehensive description.

4.2 Comparison between foetus and adult morphology

Costeur et al. [15, 20] have reconstructed the timing of growth of both the petrosal bone and the bony labyrinth of the cow. They evidenced an early ossification of the bony capsule of the inner ear, being achieved at mid gestation while the petrosal bone housing it was far from being fully ossified. Full ossification of the petrosal bone is only achieved through post-natal ontogeny and probably not before late juvenile stages when the skull adopts full adult size. This study increases our knowledge by showing that the bony pathways of the cranial nerves in the ear region are not ossified in a 6 months gestation cow. Slices through the cochlea of an even earlier stage at 4 months gestation [15] show that, while the pars cochlearis containing the cochlea ossifies first in the cow, the petrosal bone is still very porous and no structures associated to the cochlear nerve seem to be ossified yet. So ossification in the area of the modiolus occurs between the 4th and 6th months of gestation and continues to progress at the edges of the pars cochlearis through pre and post-natal ontogeny. Bone thus progressively surrounds the nerves which are most probably already connected to the soft inner ear before being encased in the petrosal bone. The adult stage shows the full ossification of the nervous pathways and spiral canal. The facial nerve enters the petrosal bone in the large hiatus Fallopii evidenced as distinct and deeply tucked within the anterior tegmen tympani by O'Leary [30]. It then runs through a thick tract connected to the internal acoustic meatus. We confirm O'Leary's observation [30] and add here that the hiatus Fallopii may be large as it is on this specimen NMB 1037.

5. CONCLUSIONS

To the best of our knowledge we here give for the first time a 3D reconstruction of the cranial nerve pathways and of the spiral canal of the cochlea of a living artiodactyl, the cow *Bos taurus*, in both a prenatal and adult stage. This first attempt shows how powerful micro-computed tomography is for our understanding of anatomical structures of the soft inner ear as they leave their pathways in the dense petrosal bone. This is now possible to access features of the biology of extinct animal related to their sense organs such as shown by Orliac et al. [17, 18]. We here participate in building the comparative morphological database which proves necessary to understand the arrangement of these features through the evolution of artiodactyls.

ACKNOWLEDGMENTS

This is a contribution to SNF Project 200021_159854/1. The authors acknowledge the financial support of the Swiss National Science Foundation (SNSF). Financial supports of the Swiss National Science Foundation in the frame of the R'equip initiative (316030 133802) is especially acknowledged.

REFERENCES

[1] Ades, H. W. and Engström, H., "Anatomy of the inner ear," In Autrum, H. et al. (eds), *Handbook of Sensory Physiology, V/1*, Springer Verlag, Berlin Heidelberg New York, 125-158 (1974).

[2] Axelssson, A., "The vascular anatomy of the cochlea of the guinea pig and man," *Acta Otolaryng.* **243**, 1-134 (1968).

[3] Axelssson, A., "The vascular anatomy of the Rhesus monkey cochlea," *Acta Otolaryng.* **77**, 381-392 (1974a).

[4] Axelssson, A., "The blood supply of the inner ear of mammals," In Autrum, H. et al. (eds), *Handbook of Sensory Physiology, V/1*, Springer Verlag, Berlin Heidelberg New York, 213-259 (1974b).

[5] Evans, E. F., "Cochlear nerve and cochlear nucleus," In Autrum, H. et al. (eds), *Handbook of Sensory Physiology, V/2*, Springer Verlag, Berlin Heidelberg New York, 1-108 (1975).

[6] Gray, H., "*Henry Gray's Anatomy of the Human Body*," Lea and Febiger, Philadelphia (1918).

[7] Fleischer, G., "Studien am Skelett des Gehörorgans der Saügetiere, einschließlich des Menschen," *Saügetierk. Mitt.* **21**,131–239 (1973).

[8] Spoor, F., Bajpai, S., Hussain, S. T., Kumar, K., and Thewissen, J. G. M., "Vestibular evidence for the evolution of aquatic behavious in early cetaceans," *Nature* **417**, 163-166 (2002).

[9] Spoor, F., Garland ,T., Krovitz, G., Ryan, T. M,, Silcox, M. T., and Walker, A., "The primate semicircular canal system and locomotion," *Proc. Natl. Acad. Sci. USA* **104**, 10808–10812 (2007).

[10] Sánchez-Villagra, M. R. and Schmelzle, T., "Anatomy and develpment of the bony inner ear in the wooly opossum, *Caluromys philander* (Didelphimorphia, Marsupiala)," *Mastozool. Neotrop.* **14**, 53–60 (2007).

[11] Ekdale, E. G., "Comparative anatomy of the bony labyrinth (inner ear) of placental mammals," *PloS ONE* **8(6)**, 1–100 (2013).

[12] Macrini, T. E., Flynn, J. J., Ni, X., Croft, D. A., and Wyss, A. R., "Comparative study of notoungulate (Placentalia, Mammalia) bony labyrinths and new phylogenetically informative inner ear characters," *J. Anat.* **223(5)**, 442–461 (2013).

[13] Mennecart, B. and Costeur, L., "Shape variation and ontogeny of the ruminant bony labyrinth, an example in Tragulidae," *J. Anat.* **229(3)**, 422–35 (2016).

[14] Thean, T., Kardjilov, N., Asher, R. J., "Inner ear development in cetaceans," *J. Anat.* **230(2)**, 249-261 (2016).

[15] Costeur, L., Mennecart, B., Müller, B., and Schulz, G., "Prenatal growth stages show the development of the ruminant bony labyrinth and petrosal bone," *J. Anat.* **230(2)**, 347-353 (2017).

[16] Luo, Z.- X., Ruf, I., Schultz, J. A., and Martin T., "Fossil evidence on evolution of inner ear cochlea in Jurassic mammals," *Proc. R. Soc. B* **278**, 28-34 (2011).

[17] Orliac, M. J. and O'Leary, M. A., "The inner ear of *Protungulatum* (Pan-Euungulata, Mammalia)," *J. Mammal. Evol.* **23(4)**, 337-352 (2016).

[18] Orliac, M. J., Aráujo, R., and Lihoreau F., "The petrosal and bony labyrinth of *Diplobune minor*, an enigmatic Artiodactyla from the Oligocene of Western Europe," *J. Morph.* **278**(9), 1168-1184 (2017).

[19] Mourlam M. J. and Orliac M. J., "Infrasonic and ultrasonic hearing evolved after the emergence of modern whale," *Current Biol.* **27**, 1-6 (2017).

[20] Costeur, L., Mennecart, B., Müller, B., and Schulz, G., "Middle ear bones of a mid-gestation ruminant foetus extracted from X-ray computed tomography," *Proc. of SPIE* **9967**, 99671Q (2016).

[21] Shambaugh, G. E., "The distribution of blood-vessels in the labyrinth of the ear of *Sus scrofa domesticus*," *Decenn. Publ. Univ. Chicago* **10**, 137–154 (1903).

[22] Khimchenko A., Schulz G., Bikis C., Deyhle H., Chicherova N., Hieber S. E., Schweighauser G., Hench J., and Müller B., "Three-dimensional imaging of human brain tissues using absorption-contrast high-resolution X-ray tomography," *Proc. of SPIE* **10162**, 101620K (2017) .

[23] Buscema M., Schulz G., Deyhle H., Khimchenko A., Matviykiv S., Holme M. N., Hipp A., Beckmann F., Saxer T., Michaud K., and Müller B., "Histology-validated X-ray tomography for imaging human coronary arteries," *Proc. of SPIE* **9967**, 99670O (2016).

[24] Dalstra M., Schulz G., Dagassan-Berndt D., Verna C., Müller-Gerbl M., and Müller B., "Hard X-ray micro-tomography of a human head post-mortem as a gold standard to compare X-ray modalities," *Proc. of SPIE* **9967**, 99670P (2016).

[25] Robinson, A.M., Stock, S.R., Soriano, C., Xiao, X., and Richter, C.-P., "Using synchrotron X-ray phase-contrast micro-computed tomography to study tissue damage by laser irradiation," *Lasers Surg. Med.* **48**, 9, 866-877 (2016).

[26] Egbert, A. and Brunke, O., "High-resolution X-ray computed tomography for materials research," *Adv. Mat. Res.* **222**, 48-51 (2011).

[27] General Electric, Measurement and Control, "Phoenix nanotom® m 180 kV / 20 W X-ray nanoCT system for high-resolution analysis and 3D metrology, https://www.gemeasurement.com/inspection-ndt/radiographyand-computed-tomography/phoenix-nanotom-m," (26.09.2016).

[28] L. Feldkamp, L. Davis, and J. Kress, "Practical cone-beam algorithm," *J. Opt. Soc. Am.* A 1, 612-619 (1984).

[29] Mennecart, B., Rössner, G. E., Métais, G., DeMiguel, D., Schulz, G., Müller, B., and Costeur, L., "The Petrosal Bone and Bony Labyrinth of Early to Middle Miocene European Deer (Mammalia, Cervidae) Reveal their Phylogeny," *J. Morph.* **277**, 1329-1338 (2016).

[30] O'Leary, M. A., "An anatomical and phylogenetic study of the osteology of the petrosal of extant and extinct artiodactylans (Mammalia) and relatives," *Bull. Am. Mus. Nat. Hist.* **335**, 1-206 (2010).